

RESEARCH

Open Access



Development of a starch-fermenting *Zymomonas mobilis* strain for bioethanol production

Yingchi Wei¹, Jia Li², Changhui Wang¹, Jiangke Yang^{1*} and Wei Shen^{1*}

Abstract

Background Biorefinery using microorganisms to produce biofuels and value-added biochemicals derived from renewable biomass offers a promising alternative to meet our sustainable energy and environmental goals. The ethanologenic strain *Zymomonas mobilis* is considered as an excellent chassis for constructing microbial cell factories for diverse biochemicals due to its outstanding industrial characteristics in ethanol production, high specific productivity, and Generally Recognized as Safe (GRAS) status. Nonetheless, the restricted substrate range constrains its application.

Results The truncated ice nucleation protein InaK from *Pseudomonas syringae* was used as an autotransporter passenger, and α -amylase was fused to the C-terminal of InaK to equip the ethanol-producing bacterium with the capability to ferment renewable biomass. Western blot and flow cytometry analysis confirmed that the amylase was situated on the outer membrane. Whole-cell activity assays demonstrated that the amylase maintained its activity on the cell surface. The recombinant *Z. mobilis* facilitated the hydrolysis of starch into oligosaccharides and enabled the streamlining of simultaneous saccharification and fermentation (SSF) processes. In a 5% starch medium under SSF, recombinant strains containing P_{eno} reached a maximum titer of 13.61 ± 0.12 g/L within 48 h. This represents an increase of 111.0% compared to the control strain's titer of 6.45 ± 0.25 g/L.

Conclusions By fusing the truncated ice nucleation protein InaK with α -amylase, we achieved efficient expression and surface display of the enzyme on *Z. mobilis*. This fusion protein exhibited remarkable enzymatic activity. Its presence enabled a cost-effective bioproduction process using starch as the sole carbon source, and it significantly reduced the required cycle time for SSF. This study not only provides an excellent *Z. mobilis* chassis for sustainable bioproduction from starch but also highlights the potential of *Z. mobilis* to function as an effective cellular factory for producing high-value products from renewable biomass.

Keywords Biorefinery, Ice nucleation protein, Cell display, Fuel ethanol, *Zymomonas mobilis*

Introduction

The growing demand for global energy is expected to outstrip fossil fuel supply in the coming decades, jeopardizing energy security worldwide [1]. Biorefinery of biomass-based fuels and chemicals show great potential in replacing traditional petroleum refineries and improving the global carbon balance. Microbial cell factories (MCFs) are instrumental in producing biofuels and biochemicals from renewable biomass, making

*Correspondence:

Jiangke Yang

jiangke.yang@gmail.com

Wei Shen

wei.shen@whpu.edu.cn; shenwei2219@gmail.com

¹ Institute of Synthetic Biology, School of Life and Technology, Wuhan Polytechnic University, Wuhan 430023, China

² State Key Laboratory of Biocatalysis and Enzyme Engineering, School of Life Sciences, Hubei University, Wuhan 430062, China



© The Author(s) 2024. **Open Access** This article is licensed under a Creative Commons Attribution-NonCommercial-NoDerivatives 4.0 International License, which permits any non-commercial use, sharing, distribution and reproduction in any medium or format, as long as you give appropriate credit to the original author(s) and the source, provide a link to the Creative Commons licence, and indicate if you modified the licensed material. You do not have permission under this licence to share adapted material derived from this article or parts of it. The images or other third party material in this article are included in the article's Creative Commons licence, unless indicated otherwise in a credit line to the material. If material is not included in the article's Creative Commons licence and your intended use is not permitted by statutory regulation or exceeds the permitted use, you will need to obtain permission directly from the copyright holder. To view a copy of this licence, visit <http://creativecommons.org/licenses/by-nc-nd/4.0/>.

substantial strides in curbing carbon emissions and promoting sustainable development [2].

Zymomonas mobilis is a facultative anaerobic Gram-negative ethanologenic bacterium and generally regarded as safe (GRAS). *Zymomonas mobilis* anaerobically ferments glucose, fructose and sucrose for ethanol production through the Entner-Doudoroff (ED) pathway with many desirable industrial characteristics, such as high specific glucose uptake rate and conversion efficiency, few byproducts, phage resistance, broad pH range (pH 3.5–7.5) and temperature (24 °C–40 °C) [3–6]. Given its naturally favorable physiological attributes, significant efforts have been made to develop *Z. mobilis* for diverse biochemicals, such as PHB [7], lactate [8], β -farnesene [9], acetoin [10], isobutanol [11] and 2,3-butanediol [12]. Moreover, the availabilities of enormous omics data, metabolic models, counterselectable system [13], exogenous and native CRISPR-Cas toolkits [14–16] as well as methods for biological part identification and characterization [17] make it an ideal chassis for biorefinery through metabolic engineering.

Although *Z. mobilis* has been engineered to broaden its range of fermentable substrates to pentose sugars such as xylose and arabinose, which are economic biochemical production from lignocellulosic biomass [18, 19], lignocellulosic hydrolysates and slurries have been utilized for cellulosic ethanol production [20]. However, the economically viable substrates utilized for fuel ethanol production are starch and cellulose-based feedstocks, which consist of macromolecular substances that are unable to penetrate cell interiors and are not directly utilized by various industrial microorganisms, such as *Escherichia coli* [21], *Saccharomyces cerevisiae* [22] and *Z. mobilis*. In industrial fermentation, sustainability depends on substrate price, availability, and competition. The limited substrate range and stressful inhibitory compounds in lignocellulosic hydrolysates constrains *Z. mobilis* for ethanol production from sugar- and starch-based feedstocks, leading to increased fermentation costs. Developing *Z. mobilis* that can utilize alternative, low-cost carbon sources, such as starch, is key for economic success. Starch is abundant and inexpensive, making it an ideal alternative to glucose [23].

Currently, *Z. mobilis* lacks effective pathways for recombinant protein secretion into the environment to achieve cost-effective consolidated bioprocessing (CBP). CBP is a process that can be successively performed by a single microbe strain capable of degrade sugar- and starch-based feedstocks into fermentable sugars for ethanol production [24]. Whole-cell biocatalyst presents an alternative for converting chemical compounds into desired products by addressing the limitation of substrate to pass through the cell envelope, especially

the membrane barrier [25]. Cell-surface display allows peptides and proteins to be displayed on the surface of microbial cells by fusing them with the anchoring motifs. Different surface proteins, such as flagellin, fimbriae, LamB, OmpA, peptidoglycan-associated lipoprotein, S-layer protein and ice nucleation protein have been utilized as anchoring motifs [26, 27], which offers a set of amenities that have led to its use in a wide range of biotechnological applications. Numerous anchoring proteins that facilitate surface display have been featured in *Z. mobilis*, such as EstA-autotransporter [28], Tat signal peptide [24] and signal peptide SP1086 [29], and they have been applied for specific purposes. Ice nucleation protein (INP) is an outer membrane-bound protein derived from *Pseudomonas syringae*, which induces ice crystallization in supercooled water [30]. INP is attached to the outer cell membrane via a glycosylphosphatidylinositol (GPI) anchor, it has been shown that full-length INP and various truncated forms INPs yield stable surface display [31, 32]. To the best of our knowledge, the INP surface display system has not previously been employed in *Z. mobilis*.

Anchoring of enzymes on the cell surface to perform catalysis has numerous advantages. It can enhance enzyme stability, as proteins anchored on cell surfaces are generally more stable under extreme conditions compared to their free-form counterparts. Additionally, the tethering of multiple synergistic enzymes on a single cell significantly reduces the distance between enzymes, thereby preventing long-distance mass transfer of substrates, particularly in high-solid fermentation processes [22, 33]. Furthermore, the products of enzymatic hydrolysis can be immediately absorbed and utilized by the cells, which can decrease the risk of contamination by maintaining low concentrations of these products in the extracellular environment, especially when glucose is released from biomass [33].

In this study, α -amylase from *Geobacillus stearothermophilus* was fused with truncated InaK to explore the feasibility displaying enzymes on the cell surface of *Z. mobilis*. This achievement provides an approach for *Z. mobilis* to directly ferment starch, thereby accelerating the development of *Z. mobilis* as an efficient microorganism for CBP in ethanol production. Additionally, this work provides a valuable approach for achieving CBP and illuminates new avenues for research into substrate utilization.

Materials and methods

Strains, vectors, and media

The plasmids and strains used in this study are listed in Table 1. *Escherichia coli* DH5 α was used for plasmid construction. *Z. mobilis* ZM4 was the parent strain for

Table 1 Plasmids and strains used in the study

	Description	Source
Plasmids		
pEZ15Asp	Shuttle vector contains <i>Z. mobilis</i> origin and <i>E. coli</i> origin p15A; <i>Sp^R</i> ; Biobrick-compatible	Lab stock [12]
pEZ-Amy-(His) ₆	<i>Sp^R</i> ; pEZ containing: <i>a-amylase</i> with 6×His-tag driven by constitutive promoter <i>PLacUV5</i>	Lab stock
pEZ-InaK-Amy	<i>Sp^R</i> ; pEZ containing: fusion gene of <i>InaK</i> and <i>a-amylase</i> driven by constitutive promoter <i>PLacUV5</i>	This work
pEZ-InaK-Amy-(His) ₆	<i>Sp^R</i> ; pEZ containing: fusion gene of <i>InaK</i> and <i>a-amylase</i> with 6×His-tag driven by constitutive promoter <i>PLacUV5</i>	This work
pEZ-D6-InaK-Amy-(His) ₆	<i>Sp^R</i> ; pEZ containing: 6×Aspartic acid charged peptides, fusion gene of <i>InaK</i> and <i>a-amylase</i> with 6×His-tag driven by constitutive promoter <i>PLacUV5</i>	This work
pEZ-E6-InaK-Amy-(His) ₆	<i>Sp^R</i> ; pEZ containing: 6×Glutamate charged peptides, fusion gene of <i>InaK</i> and <i>a-amylase</i> with 6×His-tag driven by constitutive promoter <i>PLacUV5</i>	This work
pEZ-K6-InaK-Amy-(His) ₆	<i>Sp^R</i> ; pEZ containing: 6×Lysine charged peptides, fusion gene of <i>InaK</i> and <i>a-amylase</i> with 6×His-tag driven by constitutive promoter <i>PLacUV5</i>	This work
pEZ-R6-InaK-Amy-(His) ₆	<i>Sp^R</i> ; pEZ containing: 6×Arginine charged peptides, fusion gene of <i>InaK</i> and <i>a-amylase</i> with 6×His-tag driven by constitutive promoter <i>PLacUV5</i>	This work
pEZ-KKR2-InaK-Amy-(His) ₆	<i>Sp^R</i> ; pEZ containing: 2×Two lysines and one arginine charged peptides, fusion gene of <i>InaK</i> and <i>a-amylase</i> with 6×His-tag driven by constitutive promoter <i>PLacUV5</i>	This work
pEZ-Peno-InaK-Amy	<i>Sp^R</i> ; pEZ containing: fusion gene of <i>InaK</i> and <i>a-amylase</i> driven by native constitutive promoter <i>Peno</i>	This work
pEZ-Ppdc-InaK-Amy	<i>Sp^R</i> ; pEZ containing: fusion gene of <i>InaK</i> and <i>a-amylase</i> driven by native constitutive promoter <i>Ppdc</i>	This work
pEZ-Pgap-InaK-Amy	<i>Sp^R</i> ; pEZ containing: fusion gene of <i>InaK</i> and <i>a-amylase</i> driven by native constitutive promoter <i>Pgap</i>	This work
Strains		
<i>E. coli</i> DH5a	<i>E. coli</i> for plasmid construction	Lab stock
<i>Z. mobilis</i> ZM4	<i>Zymomonas mobilis</i> subsp. <i>mobilis</i> ZM4 strain	Lab stock
ZM-Δ0028	ZM with deletion of <i>ZMO0028</i>	Lab stock
ZM-pEZ	ZM-Δ0028 plasmid pEZ15Asp	This work
ZM-InaK-Amy(His) ₆	ZM-Δ0028 plasmid pEZ-InaK-Amy-(His) ₆	This work
ZM-InaK-Amy	ZM-Δ0028 with plasmid pEZ-InaK-Amy	This work
ZM-Amy(His) ₆	ZM-Δ0028 with plasmid pEZ-Amy-(His) ₆	This work
ZM-D6-InaK-Amy(His) ₆	ZM-Δ0028 with plasmid pEZ-D6-InaK-Amy-(His) ₆	This work
ZM-E6-InaK-Amy(His) ₆	ZM-Δ0028 with plasmid pEZ-E6-InaK-Amy-(His) ₆	This work
ZM-K6-InaK-Amy(His) ₆	ZM-Δ0028 with plasmid pEZ-K6-InaK-Amy-(His) ₆	This work
ZM-R6-InaK-Amy(His) ₆	ZM-Δ0028 with plasmid pEZ-R6-InaK-Amy-(His) ₆	This work
ZM-KKR2-InaK-Amy(His) ₆	ZM-Δ0028 with plasmid pEZ-KKR2-InaK-Amy-(His) ₆	This work
ZM-Peno-InaK-Amy	ZM-Δ0028 with plasmid pEZ-Peno-InaK-Amy	This work
ZM-Ppdc-InaK-Amy	ZM-Δ0028 with plasmid pEZ-Ppdc-InaK-Amy	This work
ZM-Pgap-InaK-Amy	ZM-Δ0028 with plasmid pEZ-Pgap-InaK-Amy	This work

genetic modifications. *E. coli* strains were cultured in Luria–Bertani medium (LB, 10 g/L tryptone, 5 g/L yeast extract, 10 g/L NaCl) at 37 °C and *Z. mobilis* strains were cultured in rich medium (RMG5, 10 g/L yeast extract, 50 g/L glucose, 2 g/L KH₂PO₄) at 30 °C. When required, spectinomycin was used at the following final concentrations 100 µg/mL for both *E. coli* and *Z. mobilis*.

DNA manipulation techniques

Primers were designed to contain 15–20 nucleotides (nts) overlapping regions with adjacent DNA fragments. Sequences of the primers used in the study are listed in Additional file: Table S1. PCR products amplified by primer pairs were separated by gel electrophoresis,

followed by column purification, and subsequently quantified using a NanoDrop spectrophotometer (NanoDrop Technologies, Wilmington, DE, USA). Fragments and vectors were mixed in a molar ratio of 3:1, 0.5 U T5 exonuclease (NEB, USA), and 0.5 µL buffer 4 (NEB, USA) were added in a final volume of 5 µL [34]. All reagents were mixed and incubated on ice for 5 min. The DNA reaction was added to chemically competent *E. coli* cells, incubated on ice for 30 min, heat shocked for 45 s at 42 °C, and held on ice for 2 min. Subsequently, 1000 µL of LB medium (yeast extract 5 g/L, NaCl 10 g/L, tryptone 10 g/L), was added to the mixture and recovered for 45–60min at 37 °C with shaking (250 rpm). Cells were plated on LB agar plates containing appropriate

antibiotics. Recombinants were selected by colony PCR and confirmed by Sanger sequencing (Sangon Biotech, Shanghai, China).

Electroporation of *Z. mobilis*

Electro-competent *Z. mobilis* was prepared as described before with slight modifications [17]. Briefly, a single colony was inoculated into RMG5 media and grown without shaking at 30 °C for 24 h as the seed culture. The seed culture was then transferred into the screw-cap bottle. Cell culture was placed on ice for 30 min and cells were collected by centrifuging when reached an OD₆₀₀ value of 0.3–0.4. Cell pellets were washed once with ice-cold sterile water, re-centrifuged, and washed twice with pre-chilled sterilized 10% (v/v) glycerol. These pellets were resuspended in 10% glycerol at a concentration approximately 1000 folds higher than the starting culture. Competent cells were stored at –80 °C as small aliquots.

Zymomonas mobilis cells were transformed with plasmids by electroporation (Bio-Rad Gene Pulser, 0.1-cm gap cuvettes, 1.8 kV, 200 Ω, 25 μF). After electroporation, 1-mL RM medium was added to the electroporation mixture and cells were recovered at 30 °C for 3–6 h. The revived culture was plated on solid mating media containing appropriate antibiotics, and then incubated at 30 °C for 2–3 days. Recombinants were selected by colony PCR and confirmed by Sanger sequencing (Sangon Biotech, Shanghai, China).

Enzymatic activity assay

The enzyme activity of cell-surface display was quantitatively assessed by using the DNS method. Recombinant *Z. mobilis* was cultured in RMG2 medium at 30 °C for 24 h. The OD_{600nm} of the recombinant *Z. mobilis* was measured by using a UV spectrophotometer. Subsequently, the OD₆₀₀ was diluted to 1 with sterile water in a 2 mL EP tube. The α-amylase activity (U) is defined as the amount of enzyme required to hydrolyze starch and produce 1 μM of reducing sugar per minute under specific conditions. In a 2 mL EP tube containing 100 μL bacterial solution, 100 μL substrate (1% soluble starch), and 100 μL pH 4.8 Buffer were added. The mixture was then incubated in a water bath for 5 min. Then, 300 μL DNS (Solarbio, Beijing) was added to terminate the reaction, followed by boiling for 5 min, cooling, transferring to an EP tube, and adjusting the volume to 2 mL. For the control group, the bacterial solution was not added before the reaction, and added bacterial solution after adding DNS to terminate the reaction, and then immediately boiled for 5 min. Finally, the detection was carried out using a spectrophotometer at the wavelength λ = 540 nm. The instrument was adjusted to zero using the control group as a reference. The OD value of the experimental

group (3 parallel samples) was tested, and the data were recorded. Enzyme activity was calculated based on the glucose standard curve.

Batch fermentation in shake flasks

Simultaneous saccharification and fermentation (SSF) tests were carried out in 2% and 5% wheat starch medium using recombinant strain, and ZMO0028 strain with empty pEZ15asp plasmid was used as control. In addition to starch, 1% yeast extract and 100 μg/mL Spectinomycin were added to the medium and about 100U of glucoamylases (Vland Biotech, China) per gram of starch. Strains revived from glycerol stock were inoculated into 5-mL RM media containing appropriate antibiotics and grown overnight without shaking at 30 °C as the seed culture. The seed culture was then transferred into 50-mL shake flasks with 40 mL medium at an initial OD_{600nm} of 0.2. Strains were fermentation in shake flasks (33 °C, 100 rpm) with medium that filled 80% of the flask volume. Flasks were capped with gas-permeable membrane and samples were taken every 12 h to determine the concentration of ethanol and glucose by HPLC. Three technical replicates were used for each condition.

Flow cytometry analysis

The protocol used for flow cytometry assay of the promoter strength in terms of fluorescence intensity was modified slightly from a previous study [14]. Briefly, cells were washed with phosphate-buffered saline (PBS) twice and then resuspended into PBS to a concentration of 10⁷ cells/mL. 200 μL of re-suspended cells were blocked with PBSB (PBS containing 0.1% BSA) for 1 h, followed by three wash steps with PBS. Then, cells were incubated for 1 h at 4°C with mouse anti-His tag antibody (1:1000 dilution in PBSB) followed by three washing steps with PBS. Then, cells were then incubated for 1 h with secondary antibody (FITC-conjugated goat anti-mouse secondary antibody, dilution of 1:1000 in PBSB), followed by two washing steps with PBS. Finally, the antibody labeled cells were re-suspend in 0.5 mL PBS.

Cells were analyzed by flow cytometry using Beckman CytoFLEX FCM (Beckman Coulter, USA) with the PBS as the sheath fluid. The fluorescence of labeled cells was excited with the 488 nm laser and detected with FITC. To avoid rare events which could affect the population distribution, at least 20,000 events of each sample were analyzed. Data were processed via FlowJo software (FlowJo, LLC, USA) based on the user manual with the recommended parameters.

Western blot analysis

Samples from the shake flasks were harvest, and membrane proteins were enriched according to a rapid

isolation method [35]. Sodium dodecyl sulphate polyacrylamide gel electrophoresis (SDS-PAGE) was performed with a 5% stacking and a 12% running gel, followed by stained with Coomassie Brilliant Blue R-250. Molecular weight was estimated using a pre-stained protein ladder (10–170 kDa, Thermo, Lithuania).

For western blot analysis, after the electrophoresis, gels were transferred to methanol-activated PVDF membranes using the Trans-Blot® Semi-Dry Electrophoretic Transfer Cell (Bio-Rad, USA) and run for 20 min at 25 V. PVDF membranes was then blocked with 5% non-fat milk in phosphate-buffered saline with Tween 20 (PBST) for 1 h at room temperature, and subsequently fusion protein was probed with primary antibody (1:5000, Proteintech, China), respectively. Peroxidase-conjugated goat anti-Mouse IgG (1:5000, Proteintech, China) was used as secondary antibodies. Color development was performed by West Dure Extended Duration Substrate Kit (AntGene, China). All images were visualized using AI600 Imaging System (GE, USA).

High-pressure liquid chromatography (HPLC) analysis

Samples from the shake flasks were centrifuged at 13,000 rpm for 2 min at 4 °C and then supernatants were filtered through a 0.22- μ m syringe filter into HPLC vials. High-pressure liquid chromatography (HPLC) was performed using a Shimadzu HPLC system (Japan) equipped with Aminex Resin-Based Columns (Bio-Rad) and refractive index detector (RID) to quantify glucose and ethanol. The column temperature was set at 60 °C and 5 mM H₂SO₄ solution was used as the mobile phase with a flow rate of 0.5 mL/min.

Results and discussions

Construction of InaK-amylase fusion for the cell surface display in *Z. mobilis*

While starchy materials are abundant as carbon sources for fermentation, the wild-type *Z. mobilis* is inherently

incapable of utilizing starch for growth. Genome analysis of *Z. mobilis* revealed the absence of enzymes involved in starch degradation. To expand the substrate spectrum of *Z. mobilis*, a variety of hydrolase-encoding genes from other organisms have been introduced into *Z. mobilis*, including an amyglucosidase-encoding gene from *Aspergillus niger*, an α -amylase-encoding gene from *Bacillus licheniformis*, endoglucanase-encoding genes from *Bacillus subtilis*, *Erwinia chrysanthemi*, and *Pseudomonas fluorescens*. However, no or negligible enzymatic activity was observed in the resultant recombinant strains [36].

In this study, the truncated INP, referred to as InaK-N, containing only its N-terminal region, has been demonstrated the capability of cell surface display [37]. InaK-N and an acid α -amylase from *Geobacillus stearothermophilus* was selected for cell surface display. The in-fusion cloning method was used to attach the α -amylase to the C-terminal of InaK, in conjunction with the shuttle vector pEZ15Asp. The fusion protein was expressed under the control of the constitutive promoter P_{LacUV5} , and a TEV cleavage site linker was inserted between InaK and α -amylase to guarantee proper expression and conformation of the fusion protein (Fig. 1A). The recombinant plasmid was then transferred to ZM- Δ 0028, a strain with the *ZMO0028* gene knocked out, which encodes a type IV restriction-modification (R-M) system [38]. Recombinants generated hydrolysis zone on the starchy plate, indicating that the fusion protein had crossed the membrane barrier and functionally hydrolyzed extracellular starch. Recombinant strains ZM-pEZ, ZM-Amy(His)₆ and ZM-InaK-Amy(His)₆ were respectively cultivated on starch plates, and the results indicated that ZM-pEZ without amylase cannot hydrolyze starch. Meanwhile, ZM-InaK-Amy(His)₆, harboring fusion protein produced larger hydrolysis zone than ZM-Amy(His)₆, which only containing amylase (Fig. 1B). It is possible that the barrier posed by the cellular membrane impedes the secretion of amylase, leading to insufficient contact between

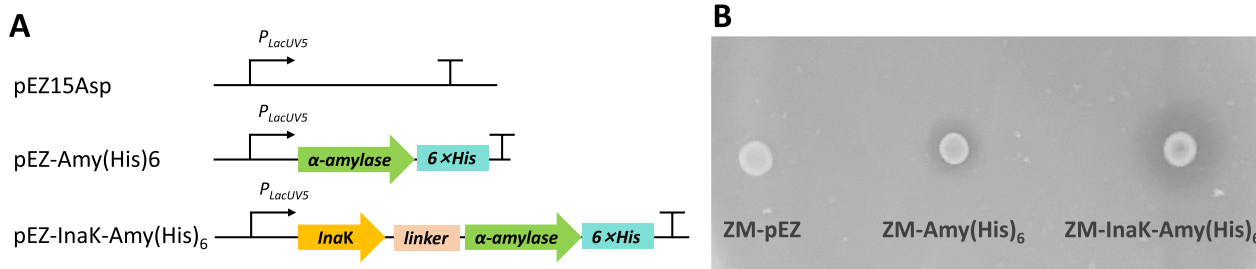


Fig. 1 The construction scheme for a starch-fermenting *Z. mobilis* strain. Scheme of cell display system employing a single plasmid approach. Genes associated with the tandem cell display system were linked by a peptide linker and driven by the constitutive promoter P_{LacUV5} , a his-tag was appended to the C-terminus (A). Hydrolysis zone generated by recombinant *Z. mobilis* in RM medium containing 2% soluble starch at 30 °C (B). At least two independent experiments were performed, yielding similar results

the amylase and the substrate without an additional signal peptide or transmembrane protein. Similar to its endogenous cellulase, this limitation could be addressed by interfering with the peptidoglycan structure of the cell walls [39]. Furthermore, it is also possible that proteins displayed on the cell surface can maintain their functions and properties more stable than free proteins, contributing to this outcome.

Confirmation of the fusion protein display on the cell surface of *Z. mobilis*

A 6×His-tag was appended to the C-terminal of α-amylase to examine its location and potential display efficiency (Fig. 2A). The localization of the fusion proteins in *Z. mobilis* was analyzed by Western Bolt. The

outer membrane proteins from the recombinant *Z. mobilis* were fractionated and followed by analysis through SDS-PAGE and Western Blot. The bands corresponding to InaK-amylase fusion protein was successfully identified in the total cell protein extracts as well as the outer membrane protein extracts (Fig. S1). Additionally, the cell surface display efficiency of recombinants was further evaluated by fluorescence-activated cell sorting (FACS) analysis (Fig. 2B). The recombinant strain InaK-Amy(His)₆ showed a display efficiency of 1.31%, while in the control cells containing empty vector pEZ15a, it was only 0.24%. Thus, it suggests that the fusion protein was successfully expressed and anchored on the membrane of *Z. mobilis*. Additionally, the introduction of signaling peptides and charged polypeptides at the N-terminal of

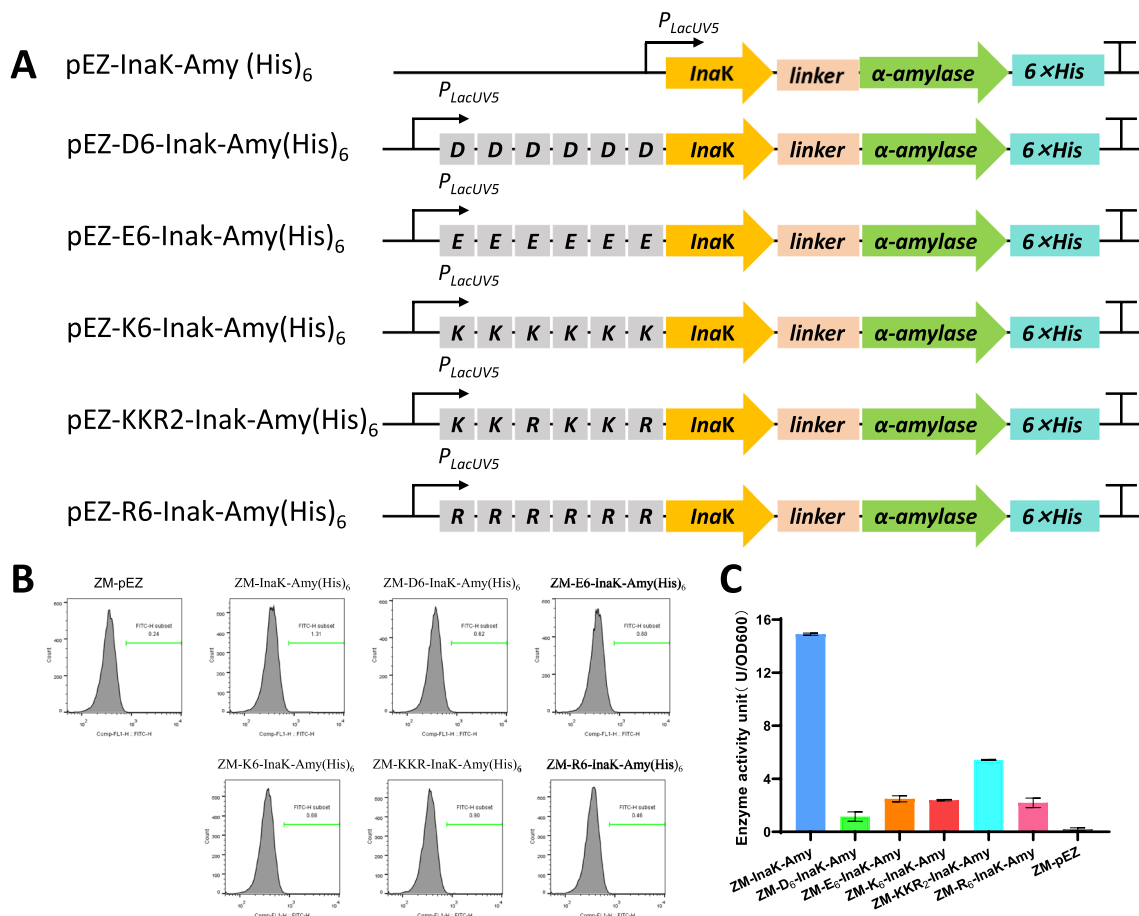


Fig. 2 Characterization of different N-terminal fusions of InaK-N with α-amylase. Constructs for fusing different InaK-Ns with α-Amylase at the C-Terminus. Genes associated with the tandem cell display system were linked by a peptide linker and driven by the constitutive promoter *P_{LacUV5}*, a his-tag was appended to the C-terminus of α-amylase (A). Flow cytometry assay for InaK-amylase. Cells containing distinct vectors, labeled with FITC-conjugated antibody against the His-tag were analyzed by flow cytometry, The excitation laser was 488nm, and the emission filter was 518nm (B). Enzyme activity assay of the recombinant *Z. mobilis* (C). Cells containing pEZ15Asp, pEZ-InaK-Amy, pEZ-E6-InaK-Amy(His)₆, pEZ-K6-InaK-Amy(His)₆, pEZ-KKR2-InaK-Amy(His)₆, pEZ-R6-InaK-Amy(His)₆ vector, respectively. A minimum of two independent experiments were conducted, all yielding comparable outcomes. Data are presented as mean ± SD (n = 3)

InaK has been observed to influence the effectiveness of cell surface display in *E. coli* [40]. Therefore, recombinants with charged polypeptides, D6-InaK-Amy(His)₆, E6-InaK-Amy(His)₆, K6-InaK-Amy(His)₆, KKR2-InaK-Amy(His)₆ were generated, respectively (Fig. 2A). These charged sequences can interact with the cell membrane or other proteins, potentially influencing the enzyme's orientation and stability on the cell surface. However, our results indicated that none of the recombinants with charged polypeptides could enhance the cell surface display efficiency of the fusion protein on the *Z. mobilis* surface, with only 0.19 to 0.88% of the total cells (Fig. 2B). This suggests that while InaK was beneficial for directing the enzyme to the cell surface, the addition of charged polypeptides may interfere with the optimal presentation of the enzyme, possibly due to electrostatic repulsion or steric hindrance.

Characterization of the surface-immobilized fusion proteins in *Z. mobilis*

The quantitative assessment of reducing sugars resulting from α -amylase enzymatic reactions was conducted using the DNS (3,5-Dinitrosalicylic acid) assay. The conditions for starch hydrolysis were determined, indicating that the optimal pH and temperature for the surface-immobilized InaK-amylase were pH 7 and 60 °C, respectively, with an enzyme activity of 45.40 ± 2.55 U/mL/OD_{600nm} (Fig. S2). However, under the optimal growth conditions for *Zymomonas mobilis* (30 °C, pH 4.8), the activity of InaK-amylase was 3.05 ± 0.41 U/mL/OD_{600nm}. Based on the experimental results above, we hypothesize that the reduced enzymatic activity could be due to two primary factors. Firstly, since amylases primarily act as high-temperature enzymes, they may not perform optimally under the growth conditions of *Z. mobilis*, as these conditions may not align with their ideal temperature

range. Secondly, the insufficient reaction speed might result from a lack of sufficient enzyme quantity, likely due to low levels of enzyme expression.

This project aims to address the problem of amylase secretion and expression by utilizing cell surface display techniques. By enhancing the display efficiency, there is a significant increase in both the enzyme's expression level and its hydrolysis efficiency. However, addressing the challenge of optimal temperature, the development of cold-active enzymes remains a critical task that to be addressed to fully resolve this issue.

Characterization of starch-fermenting *Z. mobilis* for ethanol production

To determine ethanol production of ZM-pEZ and ZM-InaK-Amy, recombinants were cultured in cooked wheat starch medium and soluble starch medium, respectively. However, no strains were able to grow, and no ethanol production was detected in the culture medium (data not show). Despite the crucial role of α -amylase in the hydrolysis of starch by efficiently cleaving α -1,4-glycosidic bonds and producing maltose and various oligosaccharides [41], *Z. mobilis* has a restricted range of substrates and is unable to thrive in a medium containing starch.

Since the conversion of starch requires the involvement of α -amylase (EC3.2.1.1) and glucoamylase (EC3.2.1.3), *Z. mobilis* lacks these enzymes. To facilitate *Z. mobilis* for ethanol production from starch, glucoamylase was attached to the C-terminal of the InaK-Amy (Fig. 3B, C). Different strategies for engineering *Z. mobilis* were employed to construct the co-display of amylase and glucoamylase. Results showed that directly linking glucoamylase to the C-terminal of α -amylase does not generate a hydrolysis zone (data not show). We speculate that the addition of glucoamylase may interfere with the structure

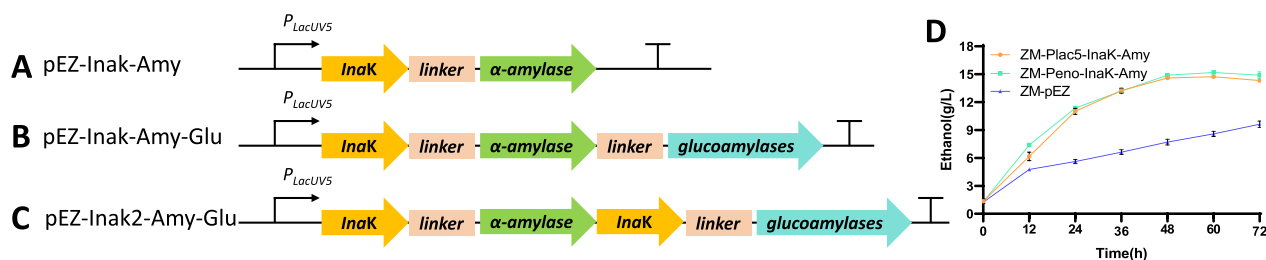


Fig. 3 Strategies for engineering *Z. mobilis* to construct simultaneous saccharification and fermentation (SSF) systems. Cell surface display system for amylase presentation in *Z. mobilis*. Genes associated with the tandem cell display system were linked by a peptide linker and driven by the constitutive promoter P_{LacUV5} (A). Co-display of amylase and glucoamylase utilizing a single InaK-N. Genes associated with the tandem cell display system were driven by P_{LacUV5} , using a single InaK-N as the anchor (B). Display of amylase and glucoamylase by dual InaK-N within a single cistron. Both amylase and glucoamylase are displayed on the cell surface by two separate InaK-N, all under the regulation of a single promoter P_{LacUV5} (C). Time-course of ethanol accumulation over 72 h. Ethanol production by recombinant *Z. mobilis* in 5% starch with glucoamylases (100 U/g starch). Cells were cultured in flasks with a shaking speed of 100 rpm at 33 °C. D At least two independent experiments were carried out with similar results. Values are the mean of one representative experiment with three or more technical replicates. Data are presented as mean \pm SD ($n=3$)

of α -amylase, potentially hindering its ability to catalyze the substrate, given that the starch-binding domain is located at the C-terminal of α -amylase [42]. Display of amylase and glucoamylase by dual InaK-N within a single cistron, where both amylase and glucoamylase are displayed on the cell surface by two separate InaK-N, and regulated by a single promoter P_{LacUV5} (Fig. 3C). The recombinant *Z. mobilis* was able to generate hydrolysis zone on a starch plate but failed to produce ethanol from starch (data not show). This may be due to inadequate display efficiency or insufficient glucoamylase activity in the recombinant strain. The glucoamylases have many certain limitations such as acidic pH requirement and slow catalytic activity [43]. Rational modification of the glucoamylase and codon optimization to increase its specific enzyme activity, along with modulation of the cellular microenvironment may address these issues. Additionally, improving the efficiency of surface display is an alternative strategy. Strategies such as promoter replacement, signal peptide optimization, cell wall modification, and adjustment of the secretory pathway can be employed [44].

To facilitate the recombinant ZM-InaK-Amy for ethanol production, glucoamylase (100 U/g starch) was added to assist in the further degradation of starch products, producing glucose to support the growth of *Z. mobilis* for simultaneous saccharification and fermentation. Fermentation of recombinants were performed in 2% and 5% cooked wheat starch media with glucoamylases, and ZM-pEZ with empty pEZ15Asp vector serving as the control. Within the initial 12 h, the ethanol production of both strains was largely consistent in media containing 2% and 5% starch. We speculate that this is due to the low biomass, glucose production exceeded bacterial glucose uptake capacity, and large specific cell surface of *Z. mobilis* together with the ED pathway facilitates glucose uptake and ethanol fermentation, as consequence, both groups yielded similar ethanol levels. After 24 h fermentation in 2% starch medium, the ethanol titer of control strain was 2.21 ± 0.12 g/L ethanol, while the recombinant strain ZM-InaK-Amy reached 3.27 ± 0.01 g/L, representing a 47.97% increase over the control. The fermentation of recombinant strains ceased around 48 h, whereas the control strain took about 60 h to reach peak ethanol production (Fig. 3B). While in 5% starch medium, as the fermentation proceeds beyond 24 h, the cell-surface-displayed amylase together supplementary glucoamylase accelerates the liquefaction of starch clumps in the fermentative milieu (Fig. S3), creating a substrate environment more favorable for glucoamylase activity, and the yield of ethanol was significantly increased, the ethanol titer was 4.38 ± 0.18 g/L and 9.67 ± 0.26 g/L with ZM-pEZ and ZM-InaK-Amy, respectively. After 36 h fermentation,

the titer of ZM-InaK-Amy reached 11.89 ± 0.21 g/L and 5.38 ± 0.21 g/L for control (Fig. 3B).

Enhancement of the expression of α -amylase to increase ethanol production

As highlighted earlier, the output of recombinant protein significantly governs the efficiency of hydrolysis, thereby directly impacting ethanol yield. To further increase ethanol production, the heterologous promoter P_{LacUV5} was substituted with native constitutive promoters of *Z. mobilis*, facilitating the construction of optimized recombinant strains. Three native constitutive promoters, P_{eno} , P_{pdc} , P_{gap} derived from *Z. mobilis* were used and generated the new recombinant strains ZM-Peno-InaK-Amy, ZM-Ppdc-InaK-Amy, ZM-Pgap-InaK-Amy, respectively (Fig. 4A). The ability of recombinants to hydrolyze starch is first tested using starch plate. The recombinants were treated as described above. The transparent zones on the starch plate demonstrated that all of the strains had the ability to hydrolyze starch, and it showed that fusion protein derived P_{eno} and P_{gap} show higher enzyme activity than P_{pdc} (Fig. 4B). ZM-Peno-InaK-Amy was used to ferment 5% wheat starch and 5% soluble starch under the previous conditions. In wheat starch, the titer of ethanol reached 13.90 ± 0.08 g/L (Fig. 3D), and in soluble starch reached 16.19 ± 0.10 g/L (Fig. 4C) within 60 h. Although the strain utilizing the native promoters have higher enzyme activity and can produce larger hydrolysis zone on the starch plate, it does not have much advantage in the ethanol yield during fermentation. We observed that the α -amylase regulated by native promoter exhibited improved ethanol production during the initial stages of fermentation. This is because the bacteria exhibit higher enzyme activity, thereby liquefying starch more rapidly. However, in the later stages of fermentation, those modified strains were able to liquefy almost all of the starch, and the fermentation rate were limited by the activity of glucoamylase.

Waste starch fermentation

Waste starch refers to the unused or residual starch that is left over from industrial processes, particularly those in the food and beverage industry. This includes spent grain from breweries, potato processing waste, pasta wastewater, or any other by-products rich in starch content. Waste starch poses environmental challenges due to its high biochemical oxygen demand (BOD) and potential to cause eutrophication if improperly disposed of. However, it also presents opportunities for recycling and valorization. Waste starch can be repurposed in various ways, such as bioconversion, energy production and animal feed.

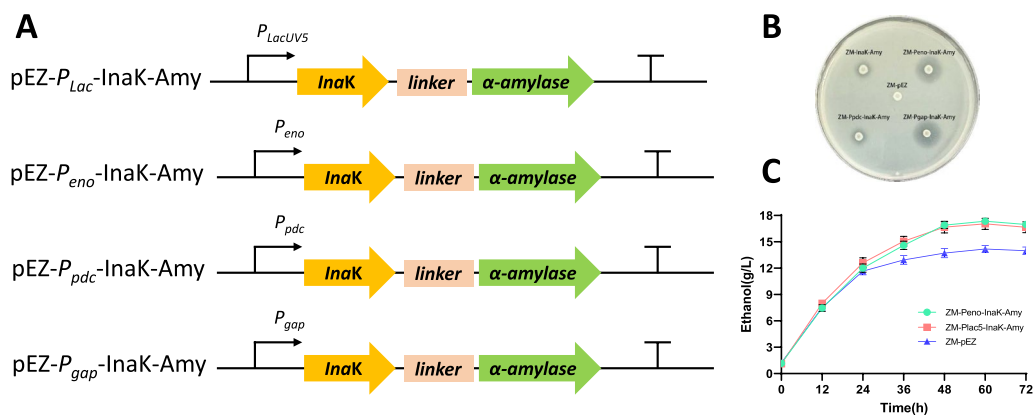


Fig. 4 Plasmid constructs for starch fermentation and their performance in recombinant strains. Strategies to enhance the efficiency of cell surface display in *Z. mobilis* through promoter replacement. Genes associated with the tandem cell display system were linked by a peptide linker and driven by different constitutive promoters P_{eno} , P_{pdc} , P_{gap} , respectively (A). The hydrolysis zone generated by recombinant *Z. mobilis* in RM medium containing 2% soluble starch at 30 °C for 48 h (B). Ethanol production by recombinant *Z. mobilis* in 5% starch with glucoamylases (100U/g). Cells were cultured in flasks with a shaking speed of 100 rpm at 33 °C (C). At least two independent experiments were carried out with similar results. Values are the mean of one representative experiment with three or more technical replicates. Data are presented as mean \pm SD (n = 3)

In present study, the recombinant strain ZM-Peno-InaK-Amy was employed to produce ethanol using waste starch. ZM-Peno-InaK-Amy was cultured in a medium containing 5% waste starch. After 24 h of cultivation, the ethanol production reached 10.40 ± 0.08 g/L. the recombinant *Z. mobilis* showed an efficient capability to ferment waste starch and convert it into bioethanol. This study not only offers a novel approach for the utilization of waste starch but also broadens the substrate range for *Z. mobilis*, making it a potential chassis organism for biotechnology applications.

Conclusion

Starch is one of the most abundant renewable materials in nature, is an inexpensive feedstock as an ideal alternative to glucose in biorefinery processes, while the low natural conversion rate of most microorganisms limits its applications. *Z. mobilis* is known for its high ethanol yield and tolerance to high alcohol concentrations, making it a desirable microbe for bioethanol production. In present study, *Z. mobilis* was developed for efficient consolidated bioprocessing of starch to ethanol. By fusing the truncated ice nucleation protein InaK with α -amylase and the addition of glucoamylase, the titer of ethanol was increased from 7.34 ± 0.23 g/L to 13.90 ± 0.08 g/L using 50 g/L of wheat starch as the substrate in 60 h. It's the first time that the INP cell surface display system has been constructed in *Z. mobilis*. The surface display of α -amylase on *Z. mobilis* can significantly reduce the amount of commercial amylase added during starchy bioethanol production, and it may even eliminate the step of high temperature liquefaction in traditional process, which effectively shortened the required cycle for

simultaneous saccharification and fermentation. Additionally, achieving the co-surface display of glucoamylase on a single cell can enhance efficiency by significantly reducing the distance between enzymes and preventing the need for long-distance substrate transfer. This approach makes the bioethanol production process more efficient, economical, and environmentally friendly. It improves the utilization of substrate materials, increases profitability, and offers a new approach for *Z. mobilis* to attain CBP, enabling direct degradation and conversion of biomass. It also paves the way for further research and development in using *Z. mobilis* and related organisms to produce high-value products from sustainable biomass.

Abbreviations

INP	Ice nucleation protein
ED	Entner-Doudoroff
HPLC	High performance liquid chromatography
RM	Rich medium
SSF	Simultaneous saccharification and fermentation
CBP	Consolidated bioprocessing
GRAS	Generally regarded as safe
MCF	Microbial cell factories
SBD	Starch binding domain

Supplementary Information

The online version contains supplementary material available at <https://doi.org/10.1186/s12934-024-02539-2>.

Additional file 1.
Additional file 2.
Additional file 3.

Acknowledgements

We thank Dr. Shihui Yang from Hubei University for helpful discussion. We thank Yongfu Yang, Binan Geng and Runxia Li for their support with High

performance liquid chromatography and insightful discussions. We also acknowledge the support from Zymobiotech (Wuhan) Co., Ltd.

Author contributions

WS conceived and designed the experiments with inputs from YW and CW. YW constructed recombinant strain and plasmids, with help from WS, JL and CW. YW and WS wrote the manuscript. WS, YW, JL, CW, and JY contributed to data analyses, read, revised and approved the final manuscript.

Funding

This work was supported by Research and Innovation Initiatives of WHPU (2024RZ012), Open Project Funding of the State Key Laboratory of Biocatalysis and Enzyme Engineering (SKLBEE20230021). Hubei Provincial Technology Innovation Program Project.

Data availability

No datasets were generated or analysed during the current study.

Declarations

Ethics approval and consent to participate

The authors declare that this study does not involve human subjects, human material and human data.

Consent for publication

All authors read and approved the final manuscript.

Competing interests

The authors declare no competing interests.

Received: 5 August 2024 Accepted: 25 September 2024

Published online: 11 November 2024

References

- Broda M, Yelle DJ, Serwańska K. Bioethanol production from lignocellulosic biomass—challenges and solutions. *Molecules*. 2022;27:8717.
- Lv X, Xue H, Qin L, Li C. Transporter engineering in microbial cell factory boosts biomanufacturing capacity. *BioDes Res*. 2022;2022:9871087.
- Wang X, He Q, Yang Y, Wang J, Haning K, Hu Y, Wu B, He M, Zhang Y, Bao J, et al. Advances and prospects in metabolic engineering of *Zymomonas mobilis*. *Metab Eng*. 2018;50:57–73.
- Yang S, Fei Q, Zhang Y, Contreras LM, Utturkar SM, Brown SD, Himmel ME, Zhang M. *Zymomonas mobilis* as a model system for production of biofuels and biochemicals. *Microb Biotechnol*. 2016;9:699–717.
- Panesar PS, Marwaha SS, Kennedy JF. *Zymomonas mobilis*: an alternative ethanol producer. *J Chem Technol Biotechnol*. 2006;81:623–35.
- Wu B, Qin H, Yang Y, Duan G, Yang S, Xin F, Zhao C, Shao H, Wang Y, Zhu Q, et al. Engineered *Zymomonas mobilis* tolerant to acetic acid and low pH via multiplex atmospheric and room temperature plasma mutagenesis. *Biotechnol Biofuels*. 2019;12:10.
- Li Y, Wang Y, Wang R, Yan X, Wang J, Wang X, Chen S, Bai F, He Q, Yang S. Metabolic engineering of *Zymomonas mobilis* for continuous co-production of bioethanol and poly-3-hydroxybutyrate (PHB). *Green Chem*. 2022;24:2588–601.
- Hu M, Bao W, Peng Q, Hu W, Yang X, Xiang Y, Yan X, Li M, Xu P, He Q, Yang S. Metabolic engineering of *Zymomonas mobilis* for co-production of D-lactic acid and ethanol using waste feedstocks of molasses and corn-cob residue hydrolysate. *Front Bioeng Biotechnol*. 2023;11:1135484.
- Xiao Y, Tan X, He Q, Yang S. Systematic metabolic engineering of *Zymomonas mobilis* for β-farnesene production. *Front Bioeng Biotechnol*. 2024;12:1392556.
- Bao W, Shen W, Peng Q, Du J, Yang S. Metabolic engineering of *Zymomonas mobilis* for acetoin production by carbon redistribution and cofactor balance. *Fermentation*. 2023;9:113.
- Qiu M, Shen W, Yan X, He Q, Cai D, Chen S, Wei H, Knoshaug EP, Zhang M, Himmel ME, Yang S. Metabolic engineering of *Zymomonas mobilis* for anaerobic isobutanol production. *Biotechnol Biofuels*. 2020;13:15.
- Yang S, Mohagheghi A, Franden MA, Chou YC, Chen X, Dowe N, Himmel ME, Zhang M. Metabolic engineering of *Zymomonas mobilis* for 2,3-butanediol production from lignocellulosic biomass sugars. *Biotechnol Biofuels*. 2016;9:189.
- Zheng Y, Fu H, Chen J, Li J, Bian Y, Hu P, Lei L, Liu Y, Yang J, Peng W. Development of a counterselectable system for rapid and efficient CRISPR. *Microb Cell Fact*. 2023;22:208.
- Shen W, Zhang J, Geng B, Qiu M, Hu M, Yang Q, Bao W, Xiao Y, Zheng Y, Peng W, et al. Establishment and application of a CRISPR-Cas12a assisted genome-editing system in *Zymomonas mobilis*. *Microb Cell Fact*. 2019;18:162.
- Zheng Y, Han J, Wang B, Hu X, Li R, Shen W, Ma X, Ma L, Yi L, Yang S, Peng W. Characterization and repurposing of the endogenous Type I-F CRISPR-Cas system of *Zymomonas mobilis* for genome engineering. *Nucl Acids Res*. 2019;47:11461–75.
- Binan G, Yalun W, Xinyan W, Yongfu Y, Peng Z, Yunhaon C, Xuan Z, Chenguang L, Fengwu B, Ping X, et al. Efficient genome-editing tools to engineer the recalcitrant non-model industrial microorganism *Zymomonas mobilis*. *Trends Biotechnol*. 2024. <https://doi.org/10.1016/j.tibtech.2024.05.005>.
- Yang Y, Shen W, Huang J, Li R, Xiao Y, Wei H, Chou Y-C, Zhang M, Himmel ME, Chen S, et al. Prediction and characterization of promoters and ribosomal binding sites of *Zymomonas mobilis* in system biology era. *Biotechnol Biofuels*. 2019;12:52.
- Zhang M, Eddy C, Deanda K, Finkelstein M, Picataggio S. Metabolic engineering of a pentose metabolism pathway in ethanologenic *Zymomonas mobilis*. *Science*. 1995;267:240–3.
- Ming XH, Bo W, Han Q, Zhi YR, Fu RT, Jing LW, Zong XS, Li CD, Qi LZ, Ke P. *Zymomonas mobilis*: a novel platform for future biorefineries. *Biotechnol Biofuels*. 2014;7:101.
- Xia J, Yang Y, Liu C-G, Yang S, Bai F-W. Engineering *Zymomonas mobilis* for robust cellulosic ethanol production. *Trends Biotechnol*. 2019;37:960–72.
- Hirose N, Kazama I, Sato R, Tanaka T, Aso Y, Ohara H. Microbial fuel cells using α-amylase-displaying *Escherichia coli* with starch as fuel. *J Biosci Bioeng*. 2021;132:519–23.
- Zhang C, Chen H, Zhu Y, Zhang Y, Li X, Wang F. *Saccharomyces cerevisiae* cell surface display technology: strategies for improvement and applications. *Front Bioeng Biotechnol*. 2022;10:1056804.
- Xia W, Zhang K, Su L, Wu J. Microbial starch debranching enzymes: developments and applications. *Biotechnol Adv*. 2021;50:107786.
- Yanase H, Nozaki K, Okamoto K. Ethanol production from cellulosic materials by genetically engineered *Zymomonas mobilis*. *Biotechnol Lett*. 2005;27:259–63.
- Schüürmann J, Quehl P, Festel G, Jose J. Bacterial whole-cell biocatalysts by surface display of enzymes: toward industrial application. *Appl Microbiol Biotechnol*. 2014;98:8031–46.
- Lee SY, Choi JH, Xu Z. Microbial cell-surface display. *Trends Biotechnol*. 2003;21:45–52.
- Kojima M, Akahoshi T, Okamoto K, Yanase H. Expression and surface display of *Cellulomonas endoglucanase* in the ethanologenic bacterium *Zymobacter palmae*. *Appl Microbiol Biotechnol*. 2012;96:1093–104.
- Tozakidis IEP, Sichert S, Teese MG, Jose J. Autotransporter mediated esterase display on *Zymomonas mobilis* and *Zymobacter palmae*. *J Biotechnol*. 2014;191:228–35.
- Luo Z, Bao J. Secretive expression of heterologous β-glucosidase in *Zymomonas mobilis*. *Bioresour Bioprocess*. 2015;2:1–6.
- Warren G, Wolber P. Molecular aspects of microbial ice nucleation. *Mol Microbiol*. 1991;5:239–43.
- Nicchi S, Giuliani M, Giusti F, Pancotto L, Maione D, Delany I, Galeotti CL, Brettoni C. Decorating the surface of *Escherichia coli* with bacterial lipoproteins: a comparative analysis of different display systems. *Microb Cell Fact*. 2021;20:33.
- Li Q, Yan Q, Chen J, He Y, Wang J, Zhang H, Yu Z, Li L. Molecular characterization of an ice nucleation protein variant (inaQ) from *Pseudomonas syringae* and the analysis of its transmembrane transport activity in *Escherichia coli*. *Int J Biol Sci*. 2012;8:1097–108.

33. Liu Z, Ho SH, Hasunuma T, Chang JS, Ren NQ, Kondo A. Recent advances in yeast cell-surface display technologies for waste biorefineries. *Biore-sour Technol.* 2016;215:324–33.
34. Yu F, Li X, Wang F, Liu Y, Zhai C, Li W, Ma L, Chen W. TLTC, a T5 exonucle-ase-mediated low-temperature DNA cloning method. *Front Bioeng Biotechnol.* 2023;11:1167534.
35. Richins RD, Kaneva I, Mulchandani A, Chen W. Biodegradation of organophosphorus pesticides by surface-expressed organophosphorus hydrolase. *Nat Biotechnol.* 1997;15:984–7.
36. Zhang K, Lu X, Li Y, Jiang X, Liu L, Wang H. New technologies provide more metabolic engineering strategies for bioethanol production in *Zymomonas mobilis*. *Appl Microbiol Biotechnol.* 2019;103:2087–99.
37. Li L, Kang DG, Cha HJ. Functional display of foreign protein on surface of *Escherichia coli* using N-terminal domain of ice nucleation protein. *Biotechnol Bioeng.* 2004;85:214–21.
38. Kerr AL, Jeon YJ, Svenson CJ, Rogers PL, Neilan BA. DNA restriction-modification systems in the ethanologen, *Zymomonas mobilis* ZM4. *Appl Microbiol Biotechnol.* 2011;89:761–9.
39. Liu P, Wu B, Chen M, Dai Y, Song C, Sun L, Huang Y, Li S, Hu G, He M. Enhancing secretion of endoglucanase in *Zymomonas mobilis* by disturbing peptidoglycan synthesis. *Appl Environ Microbiol.* 2022;88: e0216121.
40. Zhang Z, Tang R, Bian L, Mei M, Li C, Ma X, Yi L, Ma L. Surface immobiliza-tion of human arginase-1 with an engineered ice nucleation protein display system in *E. coli*. *PLoS ONE.* 2016;11: e0160367.
41. Hu YT, Hong XZ, Li HM, Yang JK, Shen W, Wang YW, Liu YH. Modifying the amino acids in conformational motion pathway of the alpha-amylase of *Geobacillus stearothermophilus* improved its activity and stability. *Front Microbiol.* 2023;14:1261245.
42. Zeng J, Guo J, Tu Y, Yuan L. Functional study of C-terminal domain of the thermoacidophilic raw starch-hydrolyzing alpha-amylase Gt-amy. *Food Sci Biotechnol.* 2020;29:409–18.
43. Kumar P, Satyanarayana T. Microbial glucoamylases: characteristics and applications. *Crit Rev Biotechnol.* 2009;29:225–55.
44. Teymennet-Ramirez KV, Martinez-Morales F, Trejo-Hernandez MR. Yeast surface display system: strategies for improvement and biotechnological applications. *Front Bioeng Biotechnol.* 2021;9:794742.

Publisher's Note

Springer Nature remains neutral with regard to jurisdictional claims in pub-lished maps and institutional affiliations.